Medicinal Chemistry
Article

J. Med. Chem. 2010, 53, 5511–5522 5511
DOI: 10.1021/jm1003667

Polyamines Inhibit Carbonic Anhydrases by Anchoring to the Zinc-Coordinated Water Molecule†

Fabrizio Carta,‡ Claudia Temperini,‡ Alessio Innocenti,‡ Andrea Scozzafava,‡ Kai Kaila,§ and Claudiu T. Supuran*,‡

‡Università degli Studi di Firenze, Polo Scientifico, Laboratorio di Chimica Bioinorganica, Rm. 188, Via della Lastruccia 3, 50019 Sesto Fiorentino (Florence), Italy, and §Department of Biosciences and Neuroscience Center, University of Helsinki, P.O. Box 65, 000140 Helsinki, Finland

Received December 15, 2009

Carbonic anhydrases (CAs, EC 4.2.1.1) are inhibited by sulfonamides, phenols, and coumarins. Polyamines such as spermine, spermidine, and many synthetic congeners are described to constitute a novel class of CA inhibitors (CAIs), interacting with the different CA isozymes with efficiency from the low nanomolar to millimolar range. The main structure−activity relationship for these CAIs have been delineated: the length of the molecule, number of amine moieties, and their functionalization are the main parameters controlling activity. The X-ray crystal structure of the CA II−spermine adduct allowed understanding of the inhibition mechanism. Spermine anchors to the nonprotein zinc ligand through a network of hydrogen bonds. Its distal amine moiety makes hydrogen bonds with residues Thr200 and Pro201, which further stabilize the adduct. Spermine binds differently compared to sulfonamides, phenols, or coumarins, rendering possible to develop CAIs with a diverse inhibition mechanism, profile, and selectivity for various isoforms.

Introduction

Polyamines such as spermine and spermidine are small polycationic aliphatic molecules ubiquitously found in organisms all over the phylogenetic tree (including animals, plants, fungi, archaea, and some bacteria), functioning in a variety of biological processes such as regulation of gene expression, translation, cell proliferation, modulation of cell signaling, membrane stabilization, and modulation of activities of several ion channels.[1−5] Being polycations, these molecules bind to anionic macromolecules such as DNA, RNA, and to some proteins, their homeostasis being ensured through regulation of biosynthesis, catabolism, and transport.[1−5] Polyamine catabolism was recently shown to play a dominant role in drug response, apoptosis, and the response to stressful stimuli and to contribute to the etiology of several pathological states, including cancer[6] and brain ischemia.[7] Thus, there is an increasing interest in understanding the interaction of such compounds with various macromolecules (nucleic acids, structural proteins, or enzymes) and in designing agents which interfere with these processes in order to obtain pharmacological agents with a novel mechanism of action.[6,7] It has been also reported recently that the brain levels of some of these polyamines vary greatly with the age in humans.[8] Indeed, spermine level was shown to be significantly decreased in the perirhinal cortex and increased in the postrhinal cortex with age. In the prefrontal cortex, there was age-related decrease in putrescine, whereas the spermidine and spermine levels were significantly increased with age. This study[8] demonstrated an age-related, region-specific change in polyamines in memory-associated structures, suggesting that the polyamine system dysfunction may contribute to aged-related impairments in hippocampal neurogenesis, learning, and memory.

Another system which has been shown recently to vary considerably in the aging brain[9,10] is that constituted by the carbonic anhydrase enzymes (CAs,[a] EC 4.2.1.1).[11,12] Indeed, these zinc proteins, which catalyze the hydration of carbon dioxide to bicarbonate and protons,[11] are present in high amounts in the vertebrate brain (several different isoforms of the 16 described in mammals are present in this organ, among which CA II, III, IV, VB, VII, VIII, IX, X, XII, and XIV),[12−14] where they play crucial roles in pH homeostasis, which affects neuronal excitability, neurotransmission, epileptogenesis, and learning and memory.[12−14] CA inhibitors (CAIs) and also CA activators (CAAs) have been shown to have profound consequences on brain function under physiological and pathophysiological conditions.[15−17]

All CAAs investigated up to now belong to the class of amino acids and amines.[17−21] Considering the possible involvement of these enzyme modulators in the brain function,[15,16] together with the recently discovered variation of polyamine concentrations in the aging brain,[8] we decided to investigate whether polyamines such as spermine and spermidine might act as CAAs. CAIs on the other hand belong to three main classes: (i) sulfonamides (such as acetazolamide **1** or dichlorophenamide **2**) and metal complexing anions, which coordinate to the Zn(II) in tetrahedral or trigonal bipyramidal geometries of the metal ion,[11] (ii) phenols (such as **3**),[20f] which bind to the zinc-coordinated water molecule/hydroxide ion from the active site, through a network of two hydrogen bonds,[20f,22] and (iii) the very recently reported third class of effective CAIs, the coumarins and thiocoumarins,[23] which have an inhibition mechanism indipendent of Zn(II), as they

†The coordinates of the hCA II−spermine adduct have been deposited in PDB, ID code 3KWA.

*To whom correspondence should be addressed. Phone: +39-055-4573005. Fax: +39-055-4573385. E-mail: claudiu.supuran@unifi.it.

[a] Abbreviations: CA, carbonic anhydrase; hCA, human CA; mCA, murine CA; CAI, CA inhibitor; SAR, structure−activity relationship.

Published on Web 06/30/2010

Chart 1. CA Inhibitors (CAIs) of the Sulfonamide Type, Acetazolamide AAZ **1**, Dichlorophenamide DCP **2**[a]

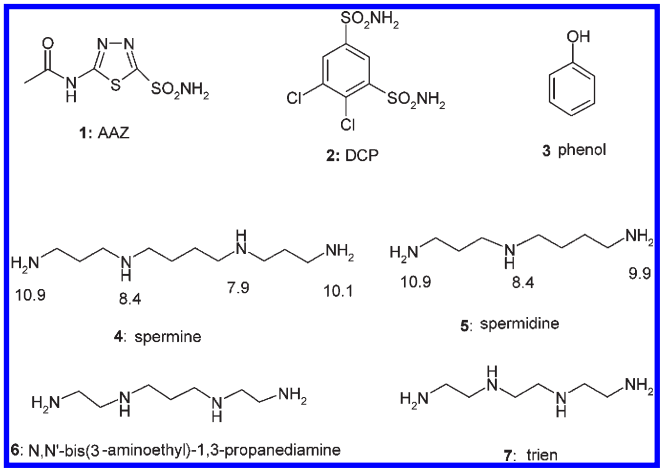

[a] Phenol **3** and the polyamines investigated here as novel CAIs include spermine **4**, spermidine **5**, *N*,*N*′-bis-(3-aminoethyl)-1,3-propanediamine **6** and triethylenetetramine (trien) **7**. pK_a values for the various amine functions of spermine and spermidine are also provided.[1]

bind (in hydrolyzed form) in the same active site region as the activators.[23] Because they do not have proton-shuttling moieties in their molecule, they occlude the active site entrance and constitute potent and isoform-selective (in some cases) inhibitors.[23] Here we report a fourth class of CA modulators, the polyamines, which unexpectedly, do not act as activators but as inhibitors of these enzymes through a novel inhibition mechanism.

Results and Discussion

Chemistry and CA Inhibition. Activators of the CAs belong to the amine and amino acid class. Both aliphatic and aromatic amines or amino acids were shown to effectively activate all CA isozymes present in mammals, i.e., CA I−CA XV.[17−20] By means of their protonatable groups, usually of the primary or secondary amine type, the CAAs facilitate the deprotonation of the water bound to the Zn(II) ion within the CA active site, with formation of the nucleophilically active species of the enzyme, with hydroxide coordinated to Zn(II) as the fourth ligand. CAIs known to date either directly bind to the Zn(II) ion from the enzyme active site (sulfonamides, inorganic complexing anions) or anchor to the nonprotein zinc ligand, a water molecule/hydroxide ion.[11] Only phenol **3** is known to inhibit CAs in this way (Chart 1).[20f,22] Recently, a third binding mode for CAIs has been reported by our group. Coumarins and thiocoumarins (in hydrolyzed form) and lacosamide bind at the entrance of the CA active site and occlude it, this inhibition mode being thus independent of the metal ion.[23]

Considering our interest in modulators (activators/inhibitors) of CA activity, and based on the rationale discussed above, polyamines such as spermine **4**, spermidine **5**, as well as many other synthetic structurally related compounds (which as outlined in the introduction, have important biological functions),[1−3] of types **6**−**21**, were assayed for their interaction with the 13 catalytically active human/murine (h/m) CA isoforms, hCA I−hCA XII, mCA XIII, hCA XIV, and mCA XV (Table 1). Our working hypothesis was that similar to other investigated amines (histamine, L-adrenaline, various heterocyclic or aromatic amines possessing aminomethyl or aminoethyl moieties).[17−20] the polycationic amines **4**−**21** may activate these CAs. Indeed, amines **4**−**9** possess several primary/secondary/tertiary amine functionalities in their molecules, with pK_as in the range of 7.9−10.9 (at least for derivatives **4** and **5**),[1] which in principle can shuttle protons from the zinc-bound water molecule to the external of the active site cavity, with formation of the nucleophilic species of CA, similarly to previously investigated amine/amino acid CAA.[17−20]

Synthetic, commercially available polyamines, such as the hexamethyl-derivative of trien **8**, 1,5-hexanediamine **9**, and its shorter analogue cadaverine **10** (1,5-pentanediamine), together with diethylenetriamine **11**, ethylenediamine, and its 1-naphthylderivative **12**, were also included in this study in order to investigate whether the length of the chain, the substitution pattern at the amino groups, and the number of heteroatoms present in the chain influence the binding to the enzymes (Chart 2). A commercially available monoderivatized spermine derivative, 1-naphthyl-acetamido-spermine **13**, has also been investigated (this synthetic analogue of the Joro spider toxin blocks calcium permeable AMPA receptors having important effects on dendrite formation by cerebellar Purkinje cells, among others),[21] together with previously prepared compounds synthesized by us, i.e., the polyamine derivatives **14**−**21**, incorporating trifluoroacetyl and *tert*-butyloxycarbonyl (Boc) protecting groups at the primary and/or secondary amino moieties of spermine (derivatives **14**−**16**) of the tetramine **6** (derivatives **17** and **18**), of trien **7** (derivatives **19** and **20**), and of 1-naphthylethylenediamine **12** (compound **21**). In this way, a rather comprehensive structure−activity relationship (SAR) insight may be gained regarding the interaction of CAs with this new class of modulators of their activity.

Inhibition data against mammalian CA isozymes CA I−XV with compounds **1**−**21** are shown in Table 1. As seen from these data, polyamines **4**−**21** do not exhibit CA activating properties against the investigated CA isoforms but, similarly to sulfonamides **1** and **2**, or phenol **3**, they show significant CA inhibitory properties. It should be noted that among polyamines investigated here, only ethylenediamine ($H_2NCH_2CH_2NH_2$) did not possess important CA inhibitory properties against any CA isoform (K_I > 500 μM, data not shown) and this compound will be not included in the subsequent discussion. The following SAR has been drawn from data of Table 1 for this new class of CAIs:

(i) Spermine **4** was a low nanomolar inhibitor (K_I of 10 nM) against hCA IV, a transmembrane isoform involved in many important physiological processes[24] and also effectively inhibited (with inhibition constants in the range of 0.71−0.99 μM) the mitochondrial isoforms hCA VA and hCA VB, the secreted one hCA VI, as well as the cytosolic hCA VII and transmembrane hCA XIV isozymes, which are present in high amounts in the human brain.[12−14] Three other CAs, i.e., hCA IX, hCA XII, and mCA XIII, were less effectively inhibited by spermine, with K_Is in the range of 13.3−27.6 μM, whereas the cytosolic, ubiquitous, and physiologically dominant hCA II and the membrane-associated one mCA XV showed K_Is in the range of 74−84 μM with this inhibitor. The least inhibited isozymes were the cytosolic hCA I and III (K_Is of 167−231 μM).

(ii) Spermidine **5**, one triamine shorter than **4** (10 carbon/nitrogen atoms in the scaffold, compared to the 14 ones of spermine), showed a CA inhibition profile quite distinct from that of spermine **4** (Table 1). hCA

Table 1. Inhibition Data with the Clinically Used Sulfonamides Acetazolamide **1**, Dichlorophenamide **2**, As Well As Phenol **3** and Polyamines **4**−**21**, against CA Isozymes I−XIV by a Stopped-Flow Technique Monitoring the CO_2 Hydration Reaction[27]

	K_I (μM)[b]						
isozyme[a]	**1**	**2**	**3**	**4**	**5**	**6**	**7**
hCA I	0.250 ± 0.01	1.20 ± 0.02	10.2 ± 0.008	231 ± 4	1.40 ± 0.06	115 ± 5	100 ± 4
hCA II	0.012 ± 0.001	0.038 ± 0.003	5.5 ± 0.01	84 ± 2	1.11 ± 0.02	75 ± 3	64 ± 1.4
hCA III	200 ± 9	680 ± 23	2.7 ± 0.03	167 ± 8	11.5 ± 0.01	63 ± 2.5	48 ± 2.1
hCA IV	0.074 ± 0.002	15 ± 0.09	9.5 ± 0.4	0.010 ± 0.001	0.112 ± 0.005	44 ± 2.1	35 ± 0.7
hCA VA	0.063 ± 0.004	0.63 ± 0.02	218 ± 10	0.84 ± 0.03	1.22 ± 0.01	50 ± 1.8	38 ± 1.1
hCA VB	0.054 ± 0.002	0.021 ± 0.001	> 500	0.83 ± 0.04	1.44 ± 0.06	59 ± 2.1	49 ± 2.4
hCA VI	0.011 ± 0.001	0.079 ± 0.006	208 ± 11	0.99 ± 0.04	1.41 ± 0.05	53 ± 2.5	43 ± 0.9
hCA VII	0.0025 ± 0.001	0.026 ± 0.002	> 500	0.71 ± 0.06	1.23 ± 0.05	58 ± 1.4	45 ± 0.8
hCA IX	0.025 ± 0.003	0.050 ± 0.004	8.8 ± 0.09	13.3 ± 0.62	1.37 ± 0.07	48 ± 2.4	39 ± 1.3
hCA XII	0.0057 ± 0.001	0.050 ± 0.002	9.2 ± 0.7	27.6 ± 1.8	44.1 ± 3.1	68 ± 3.6	57 ± 2.0
mCA XIII	0.017 ± 0.002	0.023 ± 0.001	> 500	22.6 ± 1.1	11.6 ± 0.2	66 ± 2.9	52 ± 1.1
hCA XIV	0.041 ± 0.004	0.345 ± 0.05	11.5 ± 0.7	0.86 ± 0.02	1.00 ± 0.03	36 ± 1.2	12.1 ± 0.9
mCA XV	0.072 ± 0.03	0.095 ± 0.004	10.5 ± 0.6	74 ± 3.2	10.0 ± 0.54	66 ± 1.4	59 ± 2.0
isozyme	**8**	**9**	**10**	**11**	**12**	**13**	**14**
hCA I	> 500	12.6 ± 0.9	13.3 ± 1.2	415 ± 12	> 500	12.3 ± 0.4	136 ± 9
hCA II	11.2 ± 0.09	34.4 ± 1.2	11.0 ± 0.9	118 ± 9	103 ± 9	1.13 ± 0.08	11.3 ± 0.10
hCA III	0.52 ± 0.02	0.60 ± 0.02	0.50 ± 0.02	117 ± 8	0.42 ± 0.02	11.6 ± 0.02	11.5 ± 0.08
hCA IV	0.053 ± 0.003	0.45 ± 0.01	0.052 ± 0.001	116 ± 10	0.058 ± 0.003	0.018 ± 0.002	0.116 ± 0.003
hCA VA	0.047 ± 0.001	0.61 ± 0.04	0.044 ± 0.002	110 ± 4	0.048 ± 0.002	1.03 ± 0.02	1.26 ± 0.05
hCA VB	0.71 ± 0.05	0.58 ± 0.05	0.54 ± 0.03	11.0 ± 0.9	0.061 ± 0.005	1.05 ± 0.03	1.05 ± 0.04
hCA VI	0.78 ± 0.06	0.72 ± 0.10	0.74 ± 0.06	11.5 ± 1.1	0.64 ± 0.03	0.11 ± 0.009	1.10 ± 0.02
hCA VII	0.73 ± 0.04	0.44 ± 0.03	0.42 ± 0.01	12.1 ± 0.7	0.36 ± 0.02	0.10 ± 0.007	1.09 ± 0.06
hCA IX	0.31 ± 0.009	0.41 ± 0.01	0.38 ± 0.02	10.6 ± 0.2	0.51 ± 0.04	0.12 ± 0.006	11.4 ± 0.9
hCA XII	0.52 ± 0.02	0.37 ± 0.03	0.45 ± 0.02	11.4 ± 1.1	0.38 ± 0.01	0.19 ± 0.01	10.2 ± 1.0
mCA XIII	0.58 ± 0.02	0.69 ± 0.05	0.63 ± 0.05	11.5 ± 0.5	0.62 ± 0.03	10.2 ± 0.7	12.6 ± 1.2
hCA XIV	0.74 ± 0.04	0.64 ± 0.02	0.50 ± 0.04	10.1 ± 0.8	0.59 ± 0.02	1.03 ± 0.04	6.7 ± 0.05
mCA XV	0.76 ± 0.05	0.66 ± 0.06	0.65 ± 0.02	105 ± 7	0.57 ± 0.05	0.78 ± 0.09	110 ± 3
	15	**16**	**17**	**18**	**19**	**20**	**21**
hCA I	> 500	137 ± 7	122 ± 5	> 500	> 500	> 500	> 500
hCA II	107 ± 5	110 ± 4	112 ± 7	> 500	> 500	> 500	121 ± 7
hCA III	112 ± 4	132 ± 6	96 ± 3	> 500	> 500	> 500	128 ± 8
hCA IV	104 ± 2	103 ± 2	108 ± 4	309 ± 12	> 500	> 500	12.3 ± 0.9
hCA VA	125 ± 6	131 ± 4	62 ± 1.4	416 ± 18	> 500	> 500	106 ± 4
hCA VB	103 ± 3	107 ± 3	54 ± 0.9	401 ± 15	> 500	> 500	107 ± 3
hCA VI	104 ± 3	114 ± 5	156 ± 11	> 500	> 500	> 500	109 ± 6
hCA VII	107 ± 6	108 ± 1	108 ± 9	> 500	> 500	> 500	1.24 ± 0.03
hCA IX	124 ± 3	144 ± 7	117 ± 8	> 500	> 500	> 500	12.2 ± 0.5
hCA XII	175 ± 9	165 ± 9	112 ± 5	> 500	> 500	> 500	21.5 ± 1.1
mCA XIII	179 ± 11	136 ± 4	131 ± 8	> 500	> 500	> 500	127 ± 7
hCA XIV	85 ± 2	115 ± 5	125 ± 4	> 500	> 500	> 500	34 ± 0.4
mCA XV	> 500	236 ± 14	104 ± 2	> 500	> 500	> 500	110 ± 5

[a] h = human; m = murine isozyme. [b] Mean ± standard error (n = 3, from three different assays).

IV was the most susceptible isoform to be inhibited (K_I of 112 nM). Many other CA isoforms were inhibited by **5** with inhibition constants in the low micromolar range such as hCA I, hCA II, hCA VA, hCA VB, hCA VI, hCA VII, hCA IX, and hCA XIV (K_Is in the range of 1.00−1.44 μM). Isoforms hCA III, mCA XIII, and mCA XV showed moderate inhibition with spermidine (K_Is of 10.0−11.6 μM), whereas hCA XII was the least inhibited isozyme, with K_I of 44.1 μM (Table 1).

(iii) The length of the polyamine chain seems to be an important factor governing SAR for this class of CAIs reported here. This is the reason why we investigated polyamines with a linear chain incorporating 4−14 atoms in their molecules, i.e., from ethylenediamine to spermine. The simplest polyamine, ethylenediamine ($H_2NCH_2CH_2NH_2$), did not act as a CAI against any of the 13 investigated isoforms, as mentioned above (data not shown). However, its 1-naphthyl derivative **12** showed significant CA inhibitory properties against isoforms CA III−XV, while being a rather weak hCA I and II inhibitor (K_Is of > 500 μM against hCA I and of 103 μM against hCA II). Indeed, the remaining isoforms were inhibited, with K_Is in the range of 48 nM to 0.64 μM by this simple compound (Table 1). Diamines **9** and **10** as well as the triamine **11** also showed appreciable inhibitory activity against all tested isozymes, similarly to the longer polyamines **4** (14 atoms in the chain) and **5** (10 atoms in the chain). hCA I and II were less inhibited by these amines (K_Is of 11.0−415 μM), whereas the remaining isoforms were more susceptible to inhibition, with K_Is of 44 nM to 0.74 μM (for **9** and **10**) and of 10.1−117 μM in the case of **11** (which was the least active inhibitor among the three compounds discussed here, i.e., **9**−**11**). The influence of the polyamine chain on the CA inhibitory properties can also be observed by comparing the synthesized derivatives **14**−**20**, which, as the

Chart 2. Commercially Available Polyamines **8**−**13** and Synthesized Derivatives **14**−**21** Used as CAIs in the Present Work

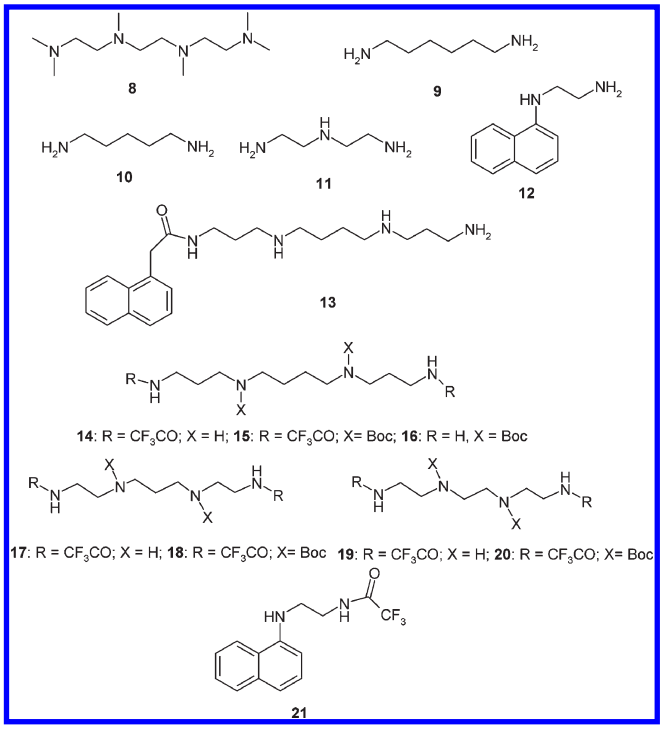

parent polyamines from which they were prepared, possess scaffolds of 10−14 atoms. Thus, the spermine derivative **14** showed good CA inhibitory properties against many isoforms (e.g., hCA IV, hCA VA, hCA VB, hCA VI, and hCA VII), whereas the shorter analogue **17** was 1−2 orders of magnitude a weaker inhibitor compared to **14**. The length of the (substituted)aliphatic scaffold incorporating from two to four amine functionalities is thus one of the principal factors influencing CA inhibitory activity of polyamines.

(iv) The number of amine moieties in the polyamine scaffold, and their substitution pattern seems to be the second critical factor influencing SAR in this new class of CAIs. We included in the study compounds possessing from two to four amine moieties. The simplest derivatives were the unsubstituted polyamines **4**−**7** and **9**−**11**, which incorporate only NH or NH_2 functionalities. However we also included **8**, which is the hexamethylated analogue of **7**, **13**, together with derivatives **14**−**20**, which have the primary, terminal amine, both the primary and secondary amine groups, and/or only the secondary amine groups derivatized by means of trifluoroacetyl or Boc moieties. It may be seen that **8** was a better CAI against all isoforms (except hCA I) compared to the nonmethylated lead **7**. The monoderivatized spermine derivative **13** was also generally more effective as a CAI compared to spermine **4**, except the activity against hCA IV, the case for which the two compounds showed similar activity (inhibition constants of 10−18 nM). In fact, **13** was one of the most promising CAIs detected so far in this work. Against hCA II, **13** was 74 times a better inhibitor compared to spermine **4**, against hCA III this factor was of 14.4, whereas against mCA XV of 94.8. Compound **21**, which incorporates trifluoroacetyl derivatized amino group (present in **12**), did show some CA inhibitory properties but highly reduced compared to **12**. Indeed, **21** inhibited efficiently only hCA VII (K_I of 1.24 μM). Thus, the presence of at least one terminal free amino group seems to be essential for inducing strong CA inhibitory properties to these molecules. By examining derivatives **14**−**20**, in which the primary and/or secondary amine moieties of spermine **4**, tetramine **6**, or trien **7** have been derivatized, this conclusion is very much reinforced. It is interesting to note that derivative **14**, which has only the primary, terminal amino moieties derivatized, still maintained some good levels of CA inhibitory activity, with K_Is in the range of 0.116−1.26 μM against isoforms hCA IV, VA, VB, VI, and VII, whereas for the remaining ones the inhibition was less strong. For the shorter derivatives **17**−**20** incorporating the same derivatization pattern discussed above, the CA inhibitory properties were very much decreased compared to the parent amines **6** and **7**, which demonstrates that not much derivatization of the amine moieties in polyamines is compatible with strong CA inhibitory properties.

(v) The investigated polyamines **4**−**21** showed an inhibition profile against the different CA isozymes different from that of other classes of CAIs. This clearly reflects the factors discussed above, which are controlling activity, i.e., the length of the polyamine chain, the number of amine functionalities present in it, and their derivatization pattern, the charged character (as ammonium cations) of these molecules, the presence of at least one bulky terminal moiety derivatizing one of the primary amino groups, etc. Indeed, the different 13 CA isoforms were inhibited with potencies ranging from the low nanomolar to the millimolar by polyamines and their derivatives, which are notably different from those of sulfonamide CAIs, such as **1**, **2**, or phenol **3** (Table 1). But the most intriguing finding was the high affinity of many polyamines for CA IV, an extracellular isoform associated to plasma membranes by phosphatidylinositol-glycan linkages, a feature unique only to this isoform among the human CAs. The most characteristic feature of the active site of this isozyme is related to the presence of four cysteine residues, which form two disulfide bonds, situated at the entrance within the active site cavity (Cys 6−Cys 11G, and Cys 23−Cys 203, respectively), which are not present in other CAs.[24a] These residues occupy the same region of the active site as the histidine residues in the cytosolic isoforms, which are involved in the binding of CAIs and CAAs.[20−25] We hypothesize that this structural feature may explain the difference in affinity for polyamine inhibitors of CA IV compared to other isoforms. As the terminal part of the polyamine inhibitor extends toward the exit of the active site cavity, where is the region with the highest variability in amino acid residues within these enzymes active sites,[23−25] it is envisageable that this new inhibition mechanism may lead to compounds with a better isoform selectivity compared to the simple derivatives investigated here, as already observed for coumarin CAIs.[23]

X-ray Crystallography and Inhibition Mechanism of Polyamines. To better understand the inhibition mechanism of

Table 2. Crystallographic Parameters and Refinement Statistics for the hCA II−Spermine **4** Adduct

Data Collection Statistics	
PDB accession number	3KWA
temperature (K)	100
wavelength (Å)	1.5418
space group	$P2_1$
unit-cell parameters (Å, deg)	a = 41.4, b = 42.1, c = 72.2, β = 104.3
total no. of measured reflections	65214
no. of unique reflections	16497
resolution (Å)	20.0−2.0
R_{sym} [a,d]	4.8% (40.0%)
$F2/\sigma(F2)$	15.1 (4.0)
completeness (%)	99.3 (99.0)
Final Model Statistics	
R_{cryst} (%) [b]	23.3
R_{free}(%) [c]	28.5
residue nos.	1−261
no. of protein atoms (including alternate conformations)	2045
no. of inhibitor atoms	14
no. of H_2O molecules	179
rmsd for bond lengths (Å), angles (deg)	0.015, 1.7
Ramachandran statistics (%): most favored, additionally allowed, and generously allowed regions	88.0, 11.6, 0.5
B factors (Å^2): average, protein, inhibitor, solvent	27.0, 14.9, 34.0, 32.1

[a] $R_{sym} = \sum |I - \langle I \rangle| / \sum \langle I \rangle$. [b] $R_{cryst} = (\sum |F_o| - |F_c| / \sum |F_{obs}|) \times 100$. [c] R_{free} is calculated in same manner as R_{cryst}, except that it uses 5% of the reflection data omitted from refinement. [d] Values in parentheses represent highest resolution shell.

this new class of CAI, the polyamines, we resolved the X-ray crystal structure (at a resolution of 2.0 Å) of spermine **4** in adduct with the physiologically dominant CA isoform, hCA II.

The crystallographic parameters and refinement statistics for the hCA II−spermine adduct are shown in Table 2. Inspection of the electron density maps (Figure 1) at various stages of the refinement, showed features compatible with the presence of one molecule of inhibitor **4** bound within the active site (Figures 1−3). All spermine atoms have a clearly defined electron density in the adduct, as shown in Figure 1, where the electron density of water113 and of the amino acid residue Gln92 are also included for reasons which will be understood shortly. The polyamine **4** (which at the pH of 7.4 at which both the kinetic and crystallographic experiments have been performed is a tetracation)[1] adopts a coiled conformation when bound to the enzyme active site, as observed from Figures 1−3. Spermine was found bound deep within the hCA II active site but not directly coordinated to the metal ion. Indeed, the Zn(II) bound water/hydroxide ion is observed both in the native hCA II and hCA II−**4** complex (Figure 1), spermine being anchored to this nonprotein zinc ligand, in a complex manner, which is reminiscent of the binding of phenol **3** to hCA II (the X-ray crystal structure for the hCA II−phenol adduct has been reported earlier).[20f] Indeed, the OH moiety of phenol makes a strong hydrogen bond (of 2.6 Å) with the nonprotein zinc ligand and a weaker one (of 3.2 Å) with the NH of Thr199, as shown schematically in Figure 4B. Spermine is anchored to the Zn(II) bound water molecule/hydroxide ion similarly to phenol **3** by means of a strong hydrogen bond of 2.8 Å involving one of its terminal ammonium groups (Figure 4A).

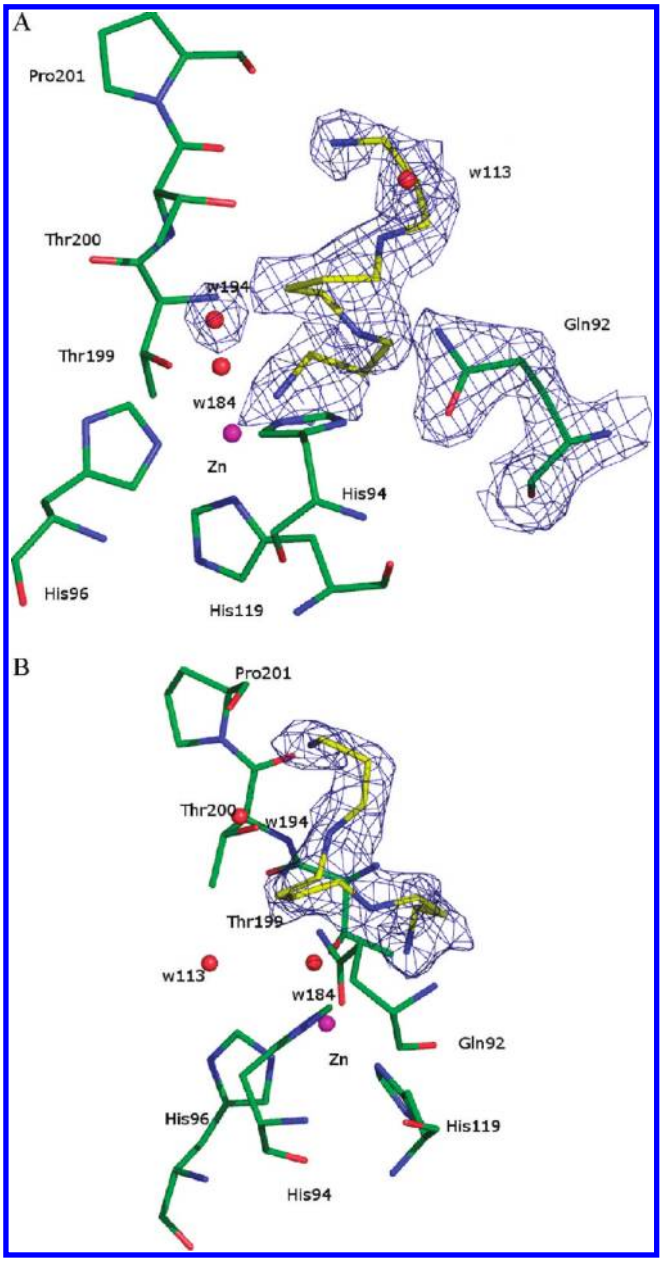

Figure 1. The electron density $2F_o - F_c$ map at 1σ of spermine (in yellow) bound within the hCA II active site (in two different orientations, A and B). The Zn(II) ion of the enzyme, its three histidine ligands (His94, 96, and 119), residues involved in the binding of the inhibitor (Thr199, Thr200, Pro201, and Gln92) as well as three water molecules participating in hydrogen bonds/van der Waals contacts with the inhibitor are also shown in A (as electron density).

If the nonprotein zinc ligand is preponderantly the hydroxide ion (as we think the situation to be at pH 7.4), one may consider the interaction between it and the ammonium moiety of spermine also as an ionic interaction. However, there are no literature data regarding the interaction of ammonium salts with negatively charged moieties present in proteins. Furthermore, the same moiety of the inhibitor (i.e., the terminal ammonium group) participates in a second hydrogen bond (of 3.0 Å) with the OH of Thr199 (and not with its amide NH, as in the hCA II−phenol adduct). The Zn(II) bound hydroxide ion makes a hydrogen bond with the same OH moiety of Thr199, which is conserved in all α-CAs for which the X-ray crystal structure has been reported so

far, in the native enzyme and in its complexes with various classes of inhibitors.[24−27] This hydrogen bond (Zn−OH-----HO-Thr199) is also present in the wild type enzyme and, together with the hydrogen bond between the carboxylate of Glu106 and the OH of Thr199, is thought to have a role in properly orienting the zinc-bound hydroxide for the nucleophilic attack on the substrates of these enzymes (CO_2, esters, coumarins, etc).[11,23−27] Thus, an important novelty of this work is that we observed for the first time the anchoring of a primary amine (as charged ammonium moiety) to the zinc-bound solvent molecule of CA, through a network of hydrogen bonds involving also the conserved amino acid residue Thr199. Although this binding has some similarity with that of phenol to the CA active site, there are also important differences between the anchoring of phenol and spermine (Figure 4A,B), as discussed above.

The two secondary amine moieties of spermine (both of them positively charged as ammonium cations at pH 7.4)[1] do

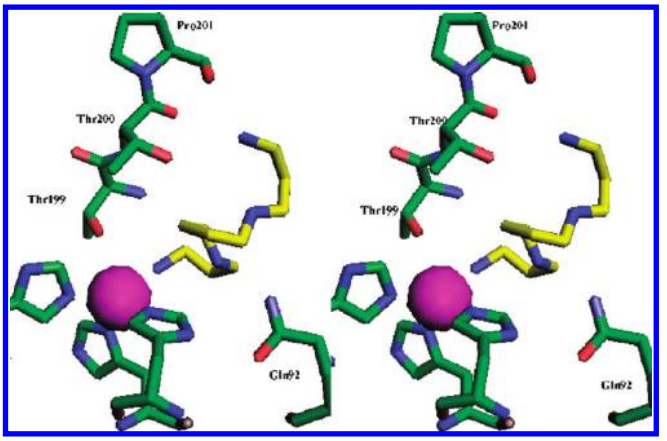

Figure 2. Stereoview of the binding of spermine (yellow) to the hCA II active site. The Zn(II) ion (violet sphere), ith three protein ligands (His94, 96 and 119) and nearby amino acid residues 92 and 199−201 are also shown.

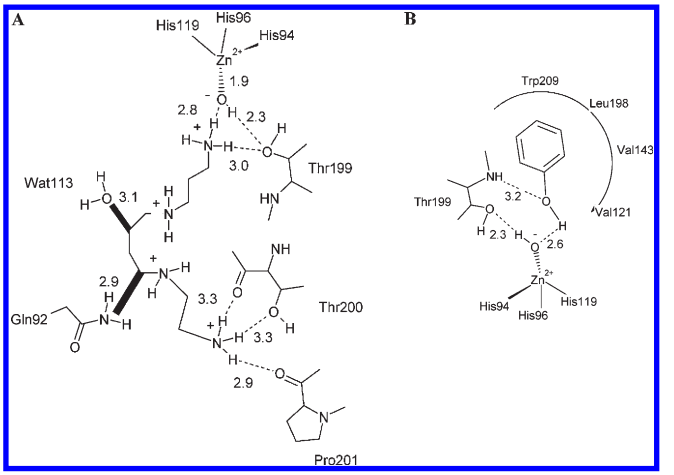

Figure 4. (A) Schematic representation of interactions in which spermine **4** (as tetracation) participates when bound to the hCA II active site. Figures represent distances (in Å). Hydrogen bonds are represented as dashed lines. In bold are shown two clashes involving some carbon atoms (C5 and C7) of the spermine scaffold with a water molecule (Wat113) and Gln92. The nonprotein zinc ligand is represented as a hydroxide ion, which should be the preponderant species at the pH at which the experiments were done (7.5). (B) Schematic representation of the binding of phenol **3**[20f] to hCA II.

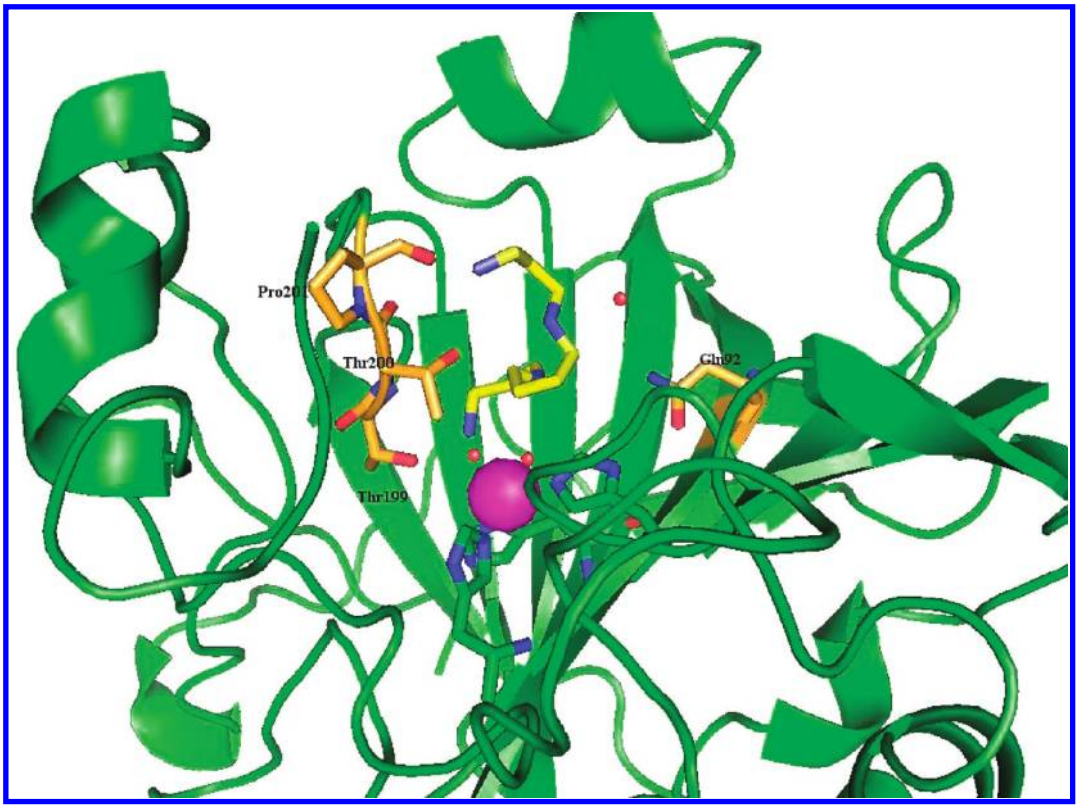

Figure 3. Detailed interactions in which spermine (in yellow) participates when bound to the hCA II active site. The zinc ion (violet sphere), the water molecule coordinated to it (small red sphere), and its three protein ligands (His94, 96, and 119, in green), as well as amino acids involved in the binding of spermine (Thr199, Thr200, Pro20,1 and Gln92, in gold) are also shown. The protein scaffold is in green (ribbon diagram).

not interact with amino acid residues of the enzyme active site (Figures 3 and 4A). The central aliphatic fragment $(CH_2)_4$ of spermine makes several weak van der Waals contacts with various amino acid residues (data not shown) and water molecules from the active site cavity, of which two are clashes with water113 (of 3.1 Å) and with the $CONH_2$ nitrogen of Gln92 (of 2.9 Å), as observed in Figures 1 and 4A. These clashes may explain the rather weak inhibitory activity of spermine against hCA II, with a K_I of 84 μM. Both propylene fragments present in spermine do not participate in any relevant contact with amino acid residues/water molecules from the enzyme active site. However, the terminal primary amine moiety (similarly to the one anchored to the zinc-bound water molecule discussed above) participates in several strong interactions with two amino acid residues known to be involved in the binding of many types of sulfonamide inhibitors,[26,28−31] i.e., Thr200 and Pro201 (Figure 4A). Thus, three hydrogen bonds of 3.3, 3.3, and 2.9 Å, respectively, have been evidenced between this ammonium moiety of spermine and the C=O of Thr200, the OH of the same amino acid residue, and the carbonyl oxygen of Pro201. All these interactions probably stabilize the enzyme−inhibitor adduct. However, the positively charged character of this inhibitor (a tetracation), the two clashes mentioned above, and the fact that it binds deep within the CA active site (without interacting with the more external part of the cavity) may explain the fact that spermine is only a weak−medium potency hCA II inhibitor (K_I of 84 μM). Indeed, there may be electrostatic repulsions between the tetracation and the metal ion from the bottom of the active site cavity, even if between the two there is the zinc-bound hydroxide, negatively charged ion. Furthermore, the inhibitor binds deep within the active site cavity, making strong contact with amino acid residues in the vicinity of the Zn(II) ion (Thr199, Thr200, and Pro201), without any contact with amino acid residues toward the exit of the cavity, as observed in Figure 5, where the hCA II−spermine adduct is superposed on the hCA II−phenol[20f] and hCA II−2-hydroxycinnamic acid[23b] adducts. These crystallographic data are in very good agreement with the solution data discussed above, as they show that there is enough space for longer or shorter polyamine analogues to bind within the active site. They also support our observations that small compact groups can derivatize the various amine functionalities of the polyamine, without the significant loss of CA inhibitory activity, but that the best inhibitors may be those possessing a terminal free amino moiety and eventually another terminal derivatized moiety, as for example in **13** (or **12**). Assuming that the long chain present in **13** will bind to the CA active site as spermine **4**, the crystallographic data show that there is enough space for the bulky terminal moiety (as the 1-naphthylacetamido one present in **13**) to be accommodated toward the exit of the active site cavity, which may lead to stronger inhibitors from this class. Indeed, the monoderivatized spermine **13** was a 74 times better hCA II inhibitor compared to spermine **4**, which is accounted for very well by our crystallographic/solution data.

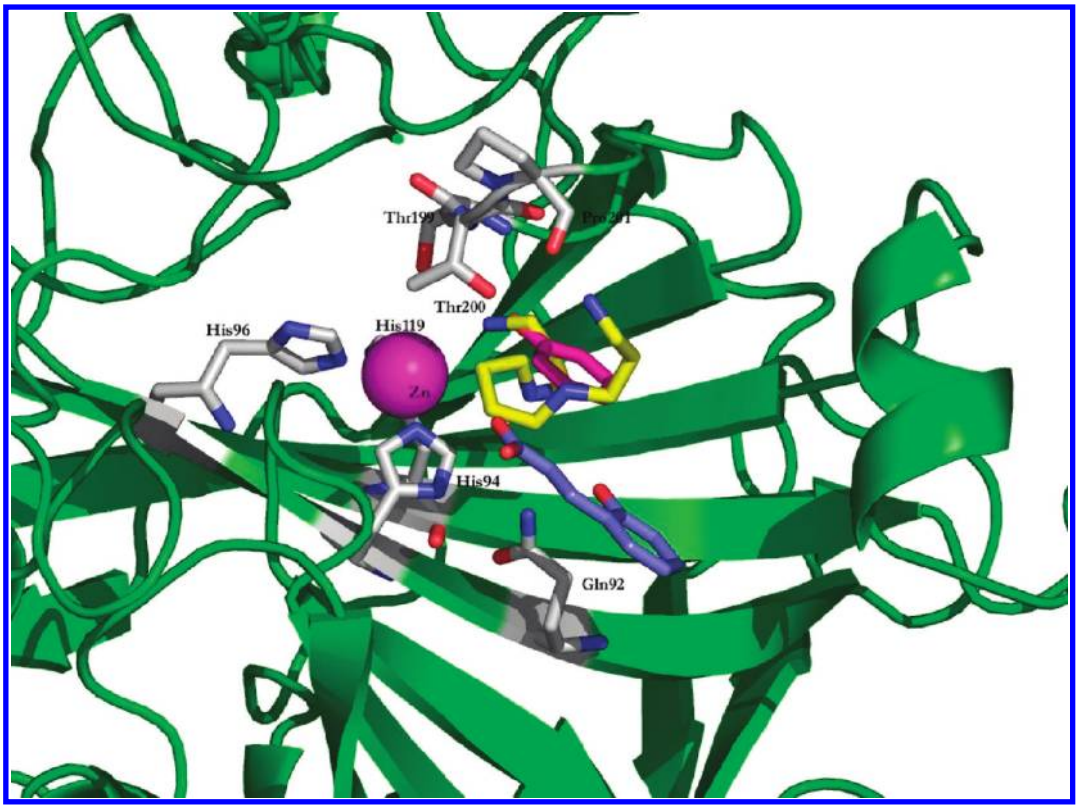

Figure 5. Superimposition of the spermine **4** (yellow), phenol **3** (magenta),[20f] and *trans*-2-hydroxycinnamic acid[23b] **22b** (violet) adducts with hCA II. The Zn(II) ion is the violet sphere. The Zn(II) histidine ligands as well as residues 92 and 199−201 involved in the binding of inhibitors are also evidenced. One terminal amino moiety of spermine (which hydrogen bonds the nonprotein zinc ligand) is fully superimposed on the phenol OH moiety, which is interacting with the same group of the enzyme. The phenyl moiety of phenol and the organic scaffold of spermine are not superimposable. 2-Hydroxycinnamic acid **22b** (in violet),[23b] the hydrolysis product of coumarin **22a** binds toward the exit of the active site and is not superposable with phenol **3** and spermine **4**.

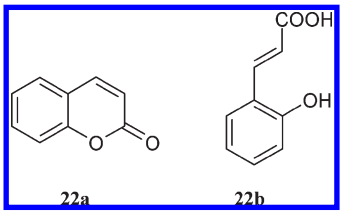

22a 22b

Returning to the comparison of this novel binding mode for a CAI, it should be noted that 2-hydroxycinnamic acid **22b**,[23b] the hydrolysis product of coumarin **22a** (in violet) binds toward the exit of the CA active site and is not superimposable with phenol **3** and spermine **4**, which are observed deep within the active site, toward the bottom of the cavity. This has important consequences for the drug design of CAIs based on these new lead molecules, the polyamines. Indeed, it is possible that by derivatization of the terminal amino moiety of spermine (or structurally related polyamines), more potent CAIs can be obtained, as there is enough space in the enzyme cavity to accommodate different moieties in the active site region where this terminal amino moiety binds (Figure 4 and 5). Another aspect of the future drug design strategies based on polyamines as lead molecules is based on the great difference in inhibitory capacity of the polyamines investigated here: small variations in the number of atoms of the chain as well as the number of heteroatoms from their molecules, strongly influence the CA inhibitory activity of these polyamines, as discussed extensively above.

Conclusions

We investigated whether polyamines such as spermine, spermidine, and some of their synthetic congeners possessing chains of 4−14 atoms, 2−4 of which are nitrogens, interfere with the CA isoforms' catalytic activity, knowing that amines and amino acids act as activators of these zinc enzymes. We report here that polyamines constitute a novel class of CAIs, inhibiting the different CA isozymes with efficiency from the low nanomolar to millimolar range. For example, spermine showed a K_I of 10 nM against CA IV, is a submicromolar inhibitor of CA VA, CA VB, CA VI, CA VII, and CA XIV, inhibits CA IX, XII, and XII in the range of 13−27 μM, and is less effective as an inhibitor of CA I, II, and III (K_Is of 84−231 μM). Spermidine, *N*,*N*′-bis-(3-aminoethyl)-1,3-propanediamine and triethylenetetramine (trien), similarly to spermine, inhibited all mammalian isozymes with very different inhibition profiles. A detailed SAR has been obtained against 13 different CA isoforms by analyzing the length of the aliphatic chain in the polyamine molecule, the number of amine functionalities, their nature (primary, secondary, or tertiary amine) and derivatization. The main SAR features have been delineated very clearly, being observed that effective CAIs may be obtained incorporating at least 7 atoms in the chain, that at least one free NH_2 moiety should be present, whereas the distal, terminal one may be functionalized even with bulkier groups. The X-ray crystal structure of the CA II−spermine adduct allowed us to understand the inhibition mechanism of CAs with polyamines and the SAR obtained by solution assays. Spermine was observed to be anchored to the nonprotein zinc ligand (a hydroxide ion at pH 7.4) through a network of hydrogen bonds involving Thr199. Furthermore, its various amine moieties made several hydrogen bonds and van der Waals contact with amino acid residues Thr200 and Pro201, which further stabilized the adduct but clashes with a water molecule and Gln92 have also been evidenced. Spermine thus binds very differently compared to sulfonamides, phenols, or coumarins within the CA active site, allowing thus for obtaining CAIs with diverse inhibition profiles and selectivity for various isoforms. Finally, it should be noted that extrapolating the above K_I values based on pure CA proteins to conditions in vivo cannot be done directly. Further work is needed to optimize these various CAIs described here to obtain compounds for in vivo studies and to develop novel drugs from these leads.

Experimental Protocols

Chemistry. Sulfonamides **1** and **2**, phenol **3**, and amines **4**−**7** are commercially available, highest purity grade reagents from Sigma-Aldrich (Milan, Italy). All CA isozymes were recombinant ones, obtained in house as reported earlier.[20,22,23] Anhydrous solvents and all reagents were purchased from Sigma-Aldrich and Alfa Aesar. All reactions involving air- or moisture-sensitive compounds were performed under a nitrogen atmosphere using dried glassware and syringes techniques to transfer solutions. Infrared (IR) spectra were recorded as thin films or nujol mulls on NaCl plates and are expressed in ν (cm^{-1}). Nuclear magnetic resonance (^1H NMR, ^{13}C NMR) spectra were determined in DMSO-d_6 and were recorded were recorded at 400 MHz on a Bruker Advance III instrument. Chemical shifts (δ scale) are reported in parts per million (ppm), and the coupling constants (J) are expressed in hertz (Hz). Splitting patterns are designated as follows: s, singlet; d, doublet; t, triplet; q, quadruplet; m, multiplet; bs, broad singlet; dd, double doublet. The assignment of exchangeable protons (O*H* and N*H*) was confirmed by the addition of D_2O. Analytical thin-layer chromatography (TLC) was carried out on Merck silica gel F-254 plates. Flash chromatography purifications were performed on Merck Silica Gel 60 (230−400 mesh ASTM) as the stationary phase. The purity has been determined by means of analytical HPLC, performed on a reversed phase C18 Bondapack column, with a Beckman EM-1760 instrument. HPLC confirmed a purity of >99.5% for the compounds investigated here.

Synthesis of N^1,N^{12}-Bis(trifluoroacetyl)spermine Bis Trifluoroacetate 14.[32]

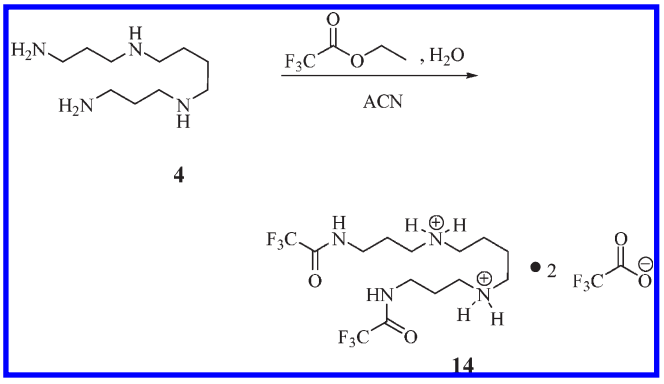

4 14

Spermine **4** (1.0 g, 1.0 equiv) was dissolved in acetonitrile (20 mL), and the clear solution was treated with ethyltrifluoroacetate (3.5 g, 5.0 equiv), water (0.2 g, 2.5 equiv), and refluxed overnight. Volatiles were removed in vacuo to give a light-brown solid that was washed with DCM (4 × 10 mL) and then purified by silica gel column chromatography eluting with 5% NH_4OH in EtOH to afford the title compound **1** as a white solid in 93% yield.

N^1,N^{12}-Bis(trifluoroacetyl)spermine Bis Trifluoroacetate (14). mp 197−199 °C (lit.[32] 195−198 °C); silica gel TLC R_f 0.50 (25% NH_4OH/EtOH); ν_{max} (KBr) cm^{-1}, 3296, 1715, 1698. δ_H (400 MHz, DMSO-d_6) 1.65 (4H, brm), 1.86 (4H, m), 2.96 (8H, brm), 3.30 (4H, m), 8.57 (4H, br, 2 × N*H*$_2$, exchange with D_2O), 9.63 (2H, br 2 × N*H*). δ_C (100 MHz, DMSO-d_6) 159.5 (q, J 32, CF_3COO^-), 157.6 (q, J 36, CF_3CON), 119.5 (q, J 156, CF_3CO), 116.0 (q, J 124,

CF_3CO), 47.0, 45.4, 37.5, 26.0, 23.6. δ_F (376 MHz, DMSO-d_6) −74.38 and −74.37 ($NHCOCF_3$), −73.6 and −73.5 (CF_3COO).

Synthesis of N^1,N^{12}-Bis(trifluoroacetyl)-N^4,N^8-bis(*t*-butoxycarbonyl)spermine 15.[33]

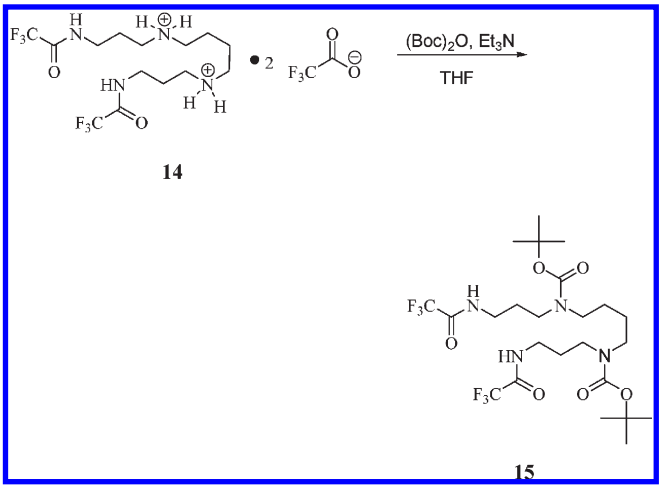

14 **15**

To a solution of N^1,N^{12}-bis(trifluoroacetyl)spermine bis trifluoroacetate **14** (1.65 g, 1.0 equiv) and triethylamine (1.61 g, 6.0 equiv) in dry THF (20 mL) was slowly added di-*tert*-butyl dicarbonate (1.74 g, 3.0 equiv) and the solution was stirred overnight at rt. The reaction was quenched with water (100 mL) and extracted with ethyl acetate (4 × 20 mL). The combined organic layers were dried over Na_2SO_4, filtered, and concentrated in vacuo to give a pale-yellow oil that was triturated with diethyl ether to afford the title compound **2** as a white solid in 78% yield.

N^1,N^{12}-Bis(trifluoroacetyl)-N^4,N^8-bis(*t*-butoxycarbonyl)spermine (15). mp 108−110 °C; silica gel TLC R_f 0.33 (1.5% MeOH/DCM); ν_{max} (KBr) cm^{-1}, 3288, 2994, 2972, 1730, 1660. δ_H (400 MHz, DMSO-d_6) 1.41 (18H, s, 6 × CH_3), 1.42 (4H, brm), 1.72 (4H, m), 3.19 (12H, m), 9.40 (2H, br, 2 × N*H*). δ_C (100 MHz, DMSO-d_6) 157.0 (q, $^3J_{C-F}$ 35), 154.8 (*C*O), 117 (q, J_{C-F} 286), 79.3 (ipso), 46.9 (d), 45.0 (d), 38.0, 28.9 (CH_3), 28.3 (d), 26.1 (d). The spectra are in agreement with reported data in the literature.[33]

Synthesis of N^4,N^8-Bis(*t*-butoxycarbonyl)spermine 16.[33]

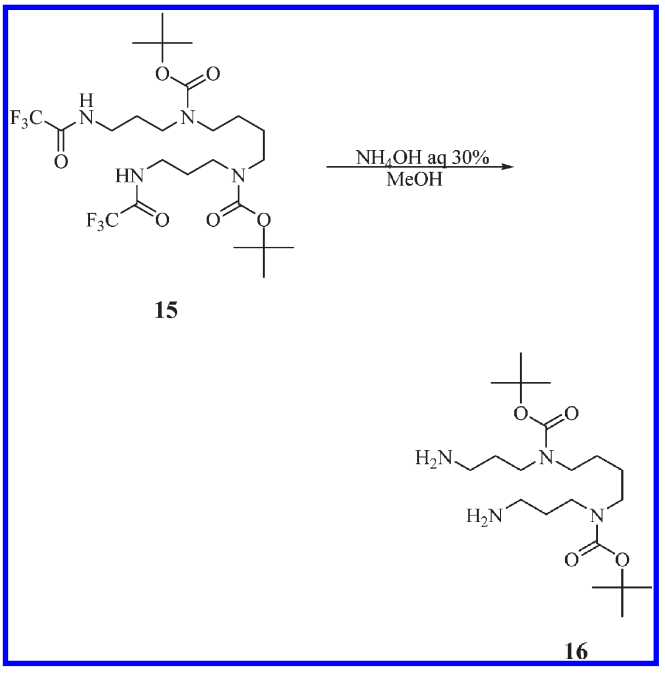

15 **16**

N^1,N^{12}-Bis-(trifluoroacetyl)-N^4,N^8-bis(*tert*-butoxycarbonyl)-spermine **15** (0.33 g) was treated with a solution (10 mL) of MeOH/NH_4OH (1/2 ratio) and the solution was stirred under reflux overnight. Then the volatiles were removed under vacuo to give a residue that was purified by silica gel column chromatography eluting with an increasing amount of MeOH in DCM from 10% to 40% to afford the titled compound **16** as a light-brown oil in 65% yield.

N^4,N^8-Bis(*t*-butoxycarbonyl)spermine (16). Silica gel TLC R_f 0.13 (25% NH_4OH/EtOH); 3434, 1656. δ_H (400 MHz, D_2O) 1.34 (9H, s, 6 × CH_3), 1.56 (4H, brs), 1.66 (4H, s, m), 2.69 (4H, m), 3.14 (8H, m). δ_C (100 MHz, D_2O) 158.1 (*C*O), 81.9 (ipso), 47.3 (br), 44.7 (br), 39.4, 38.2, 28.4, 25.6 (br). The spectra are in agreement with reported literature data.[33]

Synthesis of N^1,N^2-(2-(2,2,2-Trifluoroacetamido)ethyl)ethane-1,2-diaminium Trifluoroacetate 19.[32]

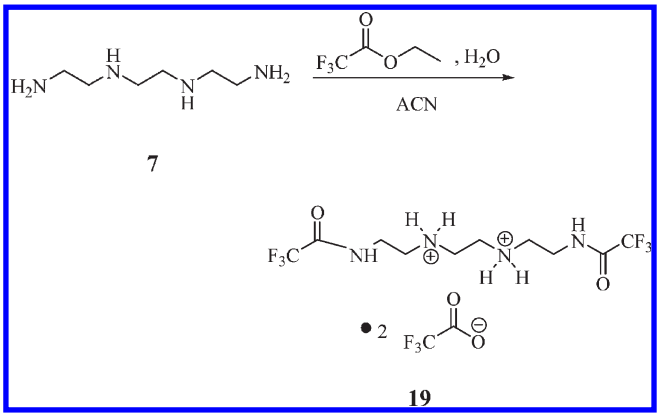

7 **19**

Triethylenetetramine (1.0 g, 1.0 equiv) was dissolved in acetonitrile (20 mL), and the clear solution was treated with ethyltrifluoroacetate (4.9 g, 5.0 equiv) and water (0.3 g, 2.5 equiv) and refluxed overnight. Volatiles were removed in vacuo to give a pale-yellow solid that was triturated with DCM to afford the title compound **19** as a white solid in 82% yield.

N^1,N^2-(2-(2,2,2-Trifluoroacetamido)ethyl)ethane-1,2-diaminium Trifluoroacetate. mp 156−1157 °C; ν_{max} (KBr) cm^{-1}, 3264, 2988, 1718, 1665. δ_H (400 MHz, DMSO-d_6) 1.97 (2H, m), 3.05 (4H, m), 3.14 (4H, m), 3.55 (4H, m), 8.93 (4H, brm, 2 × NH_2), 9.69 (2H, t, *J* 5.2) 2 × N*H*). δ_C (100 MHz, DMSO-d_6) 159.6 (q, *J* 32, CF_3COO^-), 157.8 (q, *J* 36, CF_3CON), 119.7 (q, *J* 156, CF_3CO), 114.0 (q, *J* 122, CF_3CO), 46.2, 44.9, 36.7, 23.4. δ_F (376 MHz, DMSO-d_6) −74.4, −74.6.

Synthesis of Di-*tert*-butylethane-1,2-diylbis(2-(2,2,2-trifluoroacetamido)ethylcarbamate 20.[33]

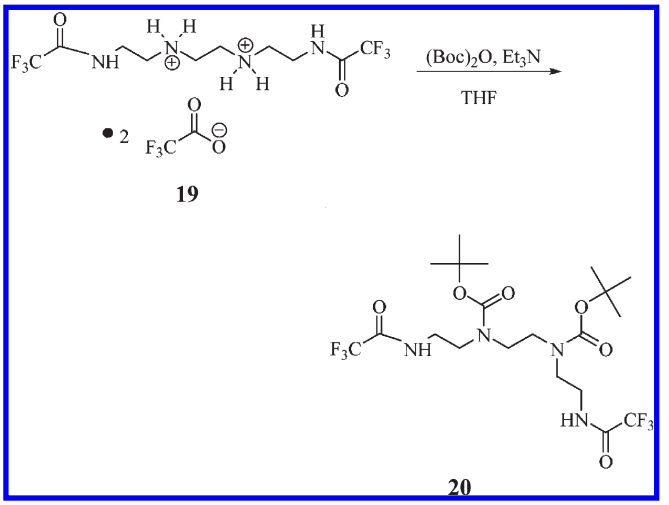

19 **20**

To a solution of N^1,N^2-(2-(2,2,2.trifluoroacetamido)ethyl)-ethane-1,2-diammonium trifluoroacetate **19** (0.2 g, 1.0 equiv) and triethylamine (0.21 g, 6.0 equiv) in dry THF (5 mL) was slowly added di-*tert*-butyl dicarbonate (0.23 g, 3.0 equiv) and

the solution was stirred overnight at rt. The reaction was quenched with an aqueous saturated solution of $NaHCO_3$ (50 mL) and extracted with DCM (3 × 20 mL). The combined organic layers were dried over Na_2SO_4, filtered, and concentrated in vacuo to give a white semisolid that was purified by silica gel column chromatography eluting with 5% MeOH in DCM to afford the titled compound **20** as a white solid in 82% yield.

Di-*tert*-Butylethane-1,2-diylbis(2-(2,2,2-trifluoroacetamido)-ethylcarbamate (20). mp 160−162 °C; silica gel TLC R_f 0.10 (5% MeOH/DCM); ν_{max} (KBr) cm^{-1}, 3270, 2988, 2970, 1720, 1664; δ_H (400 MHz, DMSO-d_6) 1.41 (18H, s, 6 × CH_3), 3.27 (12H, m), 9.50 (2H, br, 2 × NH); δ_C (100 MHz, DMSO-d_6) 157.2 (q, J 32, CF_3CON), 155.8 (CO), 116.2 (q, J 286, CF_3CO), 79.8, 45.6, 38.6, 28.8, 27.8; δ_F (376 MHz, DMSO-d_6) −74.4, −74.6.

Synthesis of N^1,N^3-bis(2-(2,2,2-trifluoroacetamido)ethyl)-propane-1,3-diaminium trifluoroacetate 17.[32]

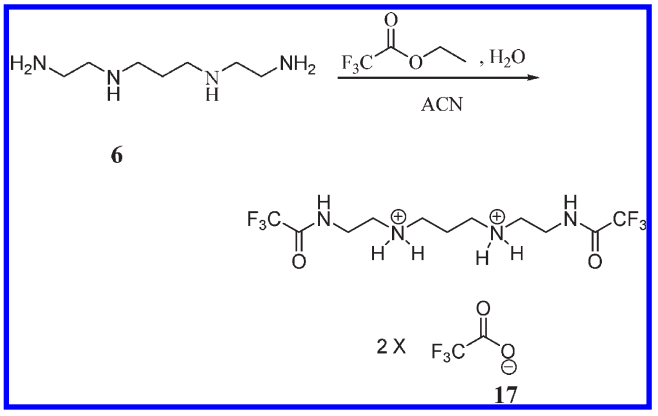

N,N^1-Bis-(2-aminoethyl)1,3-propanediamine (1.0 g, 1.0 equiv) was dissolved in acetonitrile (20 mL), and the clear solution was treated with ethyltrifluoroacetate (4.4 g, 5.0 equiv), water (0.3 g, 2.5 equiv), and refluxed overnight. Volatiles were removed in vacuo to give a white solid that was triturated with DCM to afford the title compound **17** as a white solid in 80% yield.

N^1,N^3-Bis(2-(2,2,2-trifluoroacetamido)ethyl)propane-1,3-diaminium Trifluoroacetate (17). mp 145−147 °C; ν_{max} (KBr) cm^{-1}, 3277, 2982, 2976, 1725, 1661. δ_H (400 MHz, DMSO-d_6) 1.97 (2H, m), 3.04 (4H, t, J 7.6), 3.14 (4H, t, J 6.0), 3.54 (4H, q, J 5.6), 8.93 (4H, brs, 2 × NH_2, exchange with D_2O), 9.69 (2H, t, J 5.2, 2 × NH, exchange with D_2O). δ_C (100 MHz, DMSO-d_6) 159.9 (q, J 31, CF_3COO^-), 157.6 (q, J 36, CF_3CON), 119.5 (q, J 146, CF_3CO), 116.4 (q, J 129, CF_3CO), 46.2, 44.9, 36.7, 23.3. δ_F (376 MHz, DMSO-d_6) −73.6, −74.5.

Synthesis of Di-*tert*-butylpropane-1,3-diylbis(2-(2,2,2-trifluoro-acetamido)ethylcarbamate 18.[33]

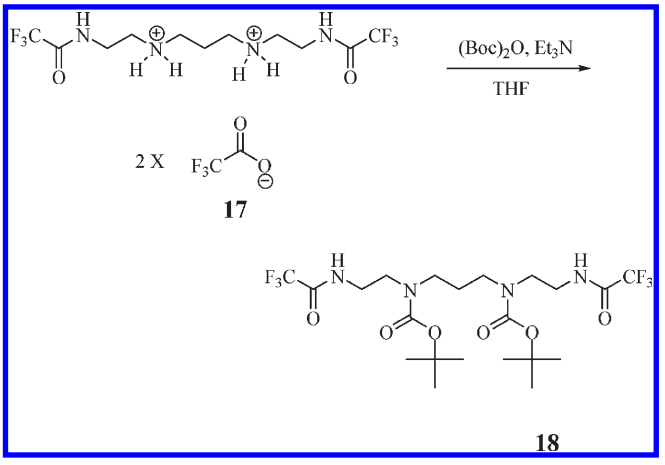

To a solution of N^1,N^3-bis(2-(2,2,2-trifluoroacetamido)ethyl)-propane-1,3-diammonium trifluoroacetate **17** (0.2 g, 1.0 equiv) and triethylamine (0.21 g, 6.0 equiv) in dry THF (3 mL) was slowly added di-*tert*-butyl dicarbonate (0.23 g, 3.0 equiv) in dry THF (2.0 mL) and the solution was stirred overnight at rt. The reaction was quenched with an aqueous saturated solution of $NaHCO_3$ (50 mL) and extracted with DCM (3 × 20 mL). The combined organic layers were dried over Na_2SO_4, filtered, and concentrated in vacuo to give a white semisolid that was triturated from diethyl ether to afford the titled compound **18** as a white solid in 87% yield.

Di-*tert*-butylpropane-1,3-diylbis(2-(2,2,2-trifluoroacetamido)-ethylcarbamate (18). mp 148−150 °C; silica gel TLC R_f 0.22 (5% MeOH/DCM); ν_{max} (KBr) cm^{-1}, 387, 2974, 2943, 1718, 1676. δ_H (400 MHz, DMSO-d_6) 1.42 (18H, s, 6 × CH_3), 1.69 (2H, m), 3.15 (4H, brm), 3.28 (8H, m). δ_C (100 MHz, DMSO-d_6) 157.4 (q, J 36, CF_3CON), 155.4 (CO) 116.0 (q, J 286, CF_3CO), 79.6, 45.5, 44.8, 38.6, 28.9, 27.8. δ_F (376 MHz, DMSO-d_6) −74.4, −74.6.

Synthesis of 2,2,2-Trifluoro-*N*-(2-(naphthalen-1-ylamino)-acetamide 21.[32]

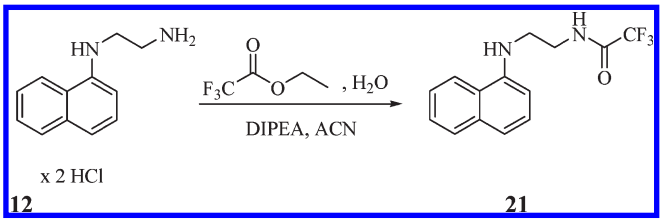

N^1-Naphthalen-1-yl)ethane-1,2-diamine dihydrochloride (0.5 g, 1.0 equiv) was suspended in acetonitrile (10 mL) and treated with ethyltrifluoroacetate (0.69 g, 5.0 equiv), water (0.04 g, 2.5 equiv), and DIPEA (0.55 g, 2.2 equiv) and refluxed overnight. Volatiles were removed in vacuo to give a sticky oil that was triturated with DCM to afford the title compound **21** as a brown solid in 86% yield.

2,2,2-Trifluoro-*N*-(2-(naphthalen-1-ylamino)acetamide (21). mp 118−120 °C; silica gel TLC R_f 0.37 (5% MeOH/DCM); ν_{max} (KBr) cm^{-1}, 3306, 2877, 1727, 1672. δ_H (400 MHz, DMSO-d_6) 3.42 (2H, q, J 5.6), 3.54 (2H, q, J 8.0), 6.32 (1H, t, J 5.6, NH, exchange with D_2O), 6.63 (1H, d, J 7.6), 7.16 (1H, d, J 8.0), 7.35 (1H, t, J 8.0), 7.46 (2H, m), 7.80 (1H, d, J 8.0), 8.12 (1H, d, J 7.6), 9.64 (1H, t, J 5.6). δ_C (100 MHz, DMSO-d_6) 157.0 (q, J 36, CF_3CON), 144.5. 135.0, 128.9, 127.7, 126.6, 125.0, 123.9, 122.4, 117.0 (q, J 286, CF_3CO), 116.7, 103.7, 42.6, 39.1. δ_F (376 MHz, DMSO-d_6) −74.4.

CA Inhibition. An Applied Photophysics stopped-flow instrument was used for assaying the CA catalyzed CO_2 hydration activity.[27] Phenol red (at a concentration of 0.2 mM) was used as indicator, working at the absorbance maximum of 557 nm, with 20 mM Hepes (pH 7.5) as buffer, and 20 mM Na_2SO_4 (for maintaining a constant ionic strength), following the initial rates of the CA-catalyzed CO_2 hydration reaction for a period of 10−100 s. The CO_2 concentrations ranged from 1.7 to 17 mM for the determination of the kinetic parameters and inhibition constants (five different substrate concentrations were used). For each inhibitor, at least six traces of the initial 5−10% of the reaction were used for determining the initial velocity. The uncatalyzed rates were determined in the same manner and subtracted from the total observed rates. Stock solutions of inhibitor (0.1 mM) were prepared in distilled−deionized water, and dilutions up to 0.01 nM were done thereafter with distilled−deionized water. Experiments were done using six different inhibitor concentrations, varying from 100 μM to 0.1 nM. Inhibitor and enzyme solutions were preincubated together for 15 min to 24 h at room temperature (15 min) or 4 °C (all other incubation times) prior to assay, in order to allow for the formation of the E−I complex or for the eventual active site mediated hydrolysis of the inhibitor. Data reported in Table 1 show the inhibition after 15 min incubation, as there were no differences of inhibitory power when the enzyme and inhibitors were kept for longer periods in incubation.[1] The inhibition constants were obtained by nonlinear least-squares methods

using PRISM 3, as reported earlier,[20,22,23] and represent the mean from at least three different determinations.

Crystallization, X-ray Data Collection, and Refinement. Crystals of the complex between hCA II and spermine **4** were obtained by using the hanging-drop method for cocrystallizing the protein with the ligand, as previously described.[20] Drops containing 5 μL of 20 mg/mL hCA II in 50 mM Tris−HCl, buffer, pH 7.4, were mixed with 5 μL of precipitant buffer (2.4 M $(NH_4)_2SO_4$ in 50 mM Tris−HCl, pH 7.4, and 1 mM sodium 4-(hydroxymercury) benzoate) with added 5 mM spermine **4** and equilibrated over a reservoir of 1 mL of precipitant buffer. A monochromatic experiment at the Cu α wavelength was performed on a crystal of hCA II grown in the presence of **4** by the rotation method on a PX-Ultra sealed-tube diffractometer (Oxford Diffraction) at 100 K. The crystal belonged to space group $P2_1$ (a = 41.4; b = 42.1; c = 72.2; β = 104.3). Data were processed with CrysAlis RED (Oxford Diffraction 2006).[28] The structure was analyzed by difference Fourier technique, using the PDB file 1CA2[25b] as starting model. The refinement was carried out with the program REFMAC5[29] model building, and map inspections were performing using the COOT program.[30] The correctness of the stereochemistry was checked using the program PROCHECK.[31] The refinement statistics of the final model of the hCA II−spermine complex are shown in Table 2.

Acknowledgment. This research was financed in part by a grant of the 6th framework programme of the European Union (DeZnIT project) and one from the 7th framework programme (Metoxia). K.K.'s work is supported by the Academy of Finland and the Sigrid Jusélius Foundation. Thanks are addressed to Dr. Giuseppina De Simone for helpful discussion with the X-ray crystallographic part of our work.

References

(1) Woster, P. M. Polyamine structure and synthetic analogs. In *Polyamine Cell Signaling, Physiology, Pharmacology and Cancer Research*; Wang, J. Y., Casero, R. A., Jr., Eds., Humana Press: Totowa, NJ, 2006; pp 3−24.

(2) Casero, R. A., Jr; Marton, L. J. Targeting polyamine metabolism and function in cancer and other hyperproliferative diseases. *Nature Rev. Drug Discovery* **2007**, *6*, 373–390.

(3) (a) Fleidervish, I. A.; Libman, L.; Katz, E.; Gutnick, M. J. Endogenous polyamines regulate cortical neuronal excitability by blocking voltage-gated Na^+ channels. *Proc. Natl. Acad. Sci. U.S.A.* **2008**, *105*, 18994–18999. (b) Wallace, H. M.; Niiranen, K. Polyamine analogues—an update. *Amino Acids* **2007**, *33*, 261–265.

(4) Soda, K.; Dobashi, Y.; Kano, Y.; Tsujinaka, S.; Konishi, F. Polyamine-rich food decreases age-associated pathology and mortality in aged mice. *Exp. Gerontol.* **2009**, *44*, 727–732.

(5) Minguet, E. G.; Vera-Sirera, F.; Marina, A.; Carbonell, J.; Blázquez, M. A. Evolutionary diversification in polyamine biosynthesis. *Mol. Biol. Evol.* **2008**, *25*, 2119–2128.

(6) Casero, R. A.; Pegg, A. E. Polyamine catabolism and disease. *Biochem. J.* **2009**, *421*, 323–338.

(7) Li, J.; Doyle, K. M.; Tatlisumak, T. Polyamines in the brain: distribution, biological interactions, and their potential therapeutic role in brain ischaemia. *Curr. Med. Chem.* **2007**, *14*, 1807–1813.

(8) Liu, P.; Gupta, N.; Jing, Y.; Zhang, H. Age-related changes in polyamines in memory-associated brain structures in rats. *Neuroscience* **2008**, *155*, 789–796.

(9) (a) Meier-Ruge, W.; Iwangoff, P.; Reichlmeier, K. Neurochemical enzyme changes in Alzheimer's disease and Pick's disease. *Arch. Gerontol. Geriatr.* **1984**, *3*, 161–165. (b) Masseguin, C.; LePanse, S.; Corman, B.; Verbavatz, J. M.; Gabrion, J. Aging affects choroidal proteins involved in CSF production in Sprague-Dawley rats. *Neurobiol. Aging* **2005**, *26*, 917–927.

(10) (a) Korolainen, M. A.; Goldsteins, G.; Nyman, T. A.; Alafuzoff, I.; Koistinaho, J.; Pirttila, T. Oxidative modification of proteins in the frontal cortex of Alzheimer's disease brain. *Neurobiol. Aging* **2006**, *27*, 42–53. (b) Sultana, R.; Poon, H. F.; Cai, J.; Pierce, W. M.; Merchant, M.; Klein, J. B.; Markesbery, W. R.; Butterfield, D. A. Identification of nitrated proteins in Alzheimer's disease brain using a redox proteomics approach. *Neurobiol. Dis.* **2006**, *22*, 76–87. (c) Izumi, M.; Yamazaki, H.; Nakabayashi, H.; Owada, M. Magnetic resonance imaging of the brain in phenylketonuria. *No To Hattatsu* **2006**, *38*, 27–31.

(11) Supuran, C. T. Carbonic anhydrases: novel therapeutic applications for inhibitors and activators. *Nature Rev. Drug Discovery* **2008**, *7*, 168–181.

(12) (a) Thiry, A.; Dogne, J. M.; Supuran, C. T.; Masereel, B. Carbonic anhydrase inhibitors as anticonvulsant agents. *Curr. Top. Med. Chem.* **2007**, *7*, 855–864. (b) Thiry, A.; Dognè, J. M.; Supuran, C. T.; Masereel, B. Anticonvulsant sulfonamides/sulfamates/sulfamides with carbonic anhydrase inhibitory activity: drug design and mechanism of action. *Curr. Pharm. Des.* **2008**, *14*, 661–671.

(13) (a) Parkkila, S.; Parkkila, A. K.; Kivela, J. Role of carbonic anhydrase and its inhibitors in biological science related to gastroenterology, neurology and nephrology. In *Carbonic Anhydrase—Its Inhibitors and Activators*, Supuran, C. T., Scozzafava, A., Conway, J., Eds.; CRC Press: Boca Raton, FL, 2004; pp 283−302; (b) Nishimori, I. Acatalytic CAs: Carbonic Anhydrase-Related Proteins. In *Carbonic Anhydrase: Its Inhibitors and Activators*; Supuran, C. T., Scozzafava, A., Conway, J., Eds.; CRC Press: Boca Raton, FL, 2004; pp 25−43.

(14) (a) Ruusuvuori, E.; Li, H.; Huttu, K.; Palva, J. M.; Smirnov, S.; Rivera, C.; Kaila, K.; Voipio, J. Carbonic anhydrase isoform VII acts as a molecular switch in the development of synchronous gamma-frequency firing of hippocampal CA1 pyramidal cells. *J. Neurosci.* **2004**, *24*, 2699–2707. (b) Rivera, C.; Voipio, J.; Kaila, K. Two developmental switches in GABAergic signalling: the K^+−Cl^- cotransporter KCC2 and carbonic anhydrase CA VII. *J. Physiol.* **2005**, *562*, 27–36.

(15) Sun, M.-K.; Alkon, D. L. Carbonic anhydrase gating of attention: memory therapy and enhancement. *Trends Pharmacol. Sci.* **2002**, *23*, 83–89.

(16) Supuran, C. T.; Scozzafava, A. Carbonic anhydrase activators as potential anti-Alzheimer's disease agents. In *Protein Misfolding in Neurodegenerative Diseases: Mechnisms and Therpeutic Strategies*; Smith, H. J., Simons, C., Sewell, R. D. E., Eds.; CRC Press, Boca Raton, FL, 2008, pp 265−288.

(17) (a) Clare, B. W.; Supuran, C. T. Carbonic anhydrase activators. Part 3. Structure−activity correlations for a series of isozyme II activators. *J. Pharm. Sci.* **1994**, *83*, 768–779. (b) Temperini, C.; Vullo, D.; Scozzafava, A.; Supuran, C. T. Carbonic anhydrase activators. Activation of isoforms I, II, IV, VA, VII, and XIV with L- and D-phenylalanine and crystallographic analysis of their adducts with isozyme II: sterospecific recognition within the active site of an enzyme and its consequences for the drug design. *J. Med. Chem.* **2006**, *49*, 3019–3027.

(18) (a) Supuran, C. T.; Scozzafava, A. Activation of carbonic anhydrase isozymes. In *The Carbonic Anhydrases−New Horizons*; Chegwidden, W. R., Carter, N., Edwards, Y., Eds.; Birkhauser Verlag: Basel, Switzerland, 2000; pp 197−219; (b) Ilies, M.; Scozzafava, A.; Supuran, C. T. Carbonic anhydrase activators. In *Carbonic anhydrase—Its Inhibitors and Activators*; Supuran, C. T., Scozzafava, A., Conway, J., Eds.; CRC Press: Boca Raton, FL, 2004; pp 317−352.

(19) (a) Scozzafava, A.; Supuran, C. T. Carbonic anhydrase activators: high affinity isozymes I, II, and IV activators, incorporating a β-alanyl-histidine scaffold. Carbonic anhydrase activators: human isozyme II is strongly activated by oligopeptides incorporating the carboxyterminal sequence of the bicarbonate anion exchanger AE1. *J. Med. Chem.* **2002**, *45*, 284–291. (b) Ilies, M.; Banciu, M. D.; Ilies, M. A.; Scozzafava, A.; Caproiu, M. T.; Supuran, C. T. Carbonic anhydrase activators: design of high affinity isozymes I, II, and IV activators, incorporating tri-/tetrasubstituted-pyridinium-azole moieties. *J. Med. Chem.* **2002**, *45*, 504–510.

(20) (a) Briganti, F.; Mangani, S.; Orioli, P.; Scozzafava, A.; Vernaglione, G.; Supuran, C. T. Carbonic anhydrase activators: X-ray crystallographic and spectroscopic investigations for the interaction of isozymes I and II with histamine. *Biochemistry* **1997**, *36*, 10384–10392. (b) Temperini, C.; Scozzafava, A.; Puccetti, L.; Supuran, C. T. Carbonic anhydrase activators: X-ray crystal structure of the adduct of human isozyme II with L-histidine as a platform for the design of stronger activators. *Biorg. Med. Chem. Lett.* **2005**, *15*, 5136–5141. (c) Temperini, C.; Scozzafava, A.; Vullo, D.; Supuran, C. T. Carbonic anhydrase activators. Activation of isozymes I, II, IV, VA, VII, and XIV with L- and D-histidine and crystallographic analysis of their adducts with isoform II: engineering proton transfer processes within the active site of an enzyme. *Chemistry* **2006**, *12*, 7057–7066. (d) Temperini, C.; Innocenti, A.; Scozzafava, A.; Mastrolorenzo, A.; Supuran, C. T. Carbonic anhydrase activators: L-Adrenaline plugs the active site entrance of isozyme II, activating better isoforms I, IV, VA, VII, and XIV. *Bioorg. Med. Chem. Lett.* **2007**, *17*, 628–635. (e) Temperini, C.; Innocenti, A.; Scozzafava, A.; Supuran, C. T. Carbonic anhydrase activators. Kinetic and X-ray crystallographic study for the interaction of D- and L-tryptophan with the mammalian isoforms I−XIV. *Bioorg. Med. Chem.* **2008**, *16*, 8373–8378. (f) Nair, S. K.; Ludwig, P. A.; Christianson, D. W. Phenol as a carbonic anhydrase inhibitor. *J. Am. Chem. Soc.* **1994**, *116*, 3659–3660.

(21) Tanaka, M.; Sakata, S.; Hirshima, N. Effects of 1-naphthyl acetyl spermine on dendrite formation by cultured cerebellar Purkinje cells. *Neurosci. Lett*. **2009**, *462*, 30–32.
(22) (a) Innocenti, A.; Vullo, D.; Scozzafava, A.; Supuran, C. T. Carbonic anhydrase inhibitors. Interactions of phenols with the 12 catalytically active mammalian isoforms (CA I−XIV). *Bioorg. Med. Chem. Lett*. **2008**, *18*, 1583–1587. (b) Innocenti, A.; Hilvo, M.; Scozzafava, A.; Parkkila, S.; Supuran, C. T. Carbonic anhydrase inhibitors. Inhibition of the new membrane-associated isoform XV with phenols. *Bioorg. Med. Chem. Lett*. **2008**, *18*, 3593–3596. (c) Innocenti, A.; Vullo, D.; Scozzafava, A.; Supuran, C. T. Carbonic anhydrase inhibitors. Inhibition of mammalian isoforms I−XIV with a series of substituted phenols including paracetamol and salicylic acid. *Bioorg. Med. Chem*. **2008**, *16*, 7424–7428. (d) Bayram, E.; Senturk, M.; Kufrevioglu, O. I.; Supuran, C. T. In vitro effects of salicylic acid derivatives on human cytosolic carbonic anhydrase isozymes I and II. *Bioorg. Med. Chem*. **2008**, *16*, 9101–9105.
(23) (a) Maresca, A.; Temperini, C.; Vu, H.; Pham, N. B.; Poulsen, S. A.; Scozzafava, A.; Quinn, R. J.; Supuran, C. T. Non-zinc mediated inhibition of carbonic anhydrases: coumarins are a new class of suicide inhibitors. *J. Am. Chem. Soc*. **2009**, *131*, 3057–3062. (b) Maresca, A.; Temperini, C.; Pochet, L.; Masereel, B.; Scozzafava, A.; Supuran, C. T. Deciphering the mechanism of carbonic anhydrase inhibition with coumarins and thiocoumarins. *J. Med. Chem*. **2010**, *53*, 335–344. (c) Temperini, C.; Innocenti, A.; Scozzafava, A.; Parkkila, S.; Supuran, C. T. The coumarin-binding site in carbonic anhydrase accommodates structurally diverse inhibitors: the antiepileptic lacosamide as an example. *J. Med. Chem*. **2010**, *53*, 850–854.
(24) (a) Sly, W. S.; Zhu., X. L.; Sato, S. CA IV from human lung and kidney: purification, characterization, and demonstration that both are anchored to membranes through a phosphatidylinositol-glycan linkage. In *Carbonic Anhydrase—From Biochemistry and Genetics to Physiology and Clinical Medicine*; Botré, F., Gros, G., Storey, B. T., Eds.; VCH: Weinheim, 1991; pp 226−231. (b) Stams, T.; Nair, S. K.; Okuyama, T.; Waheed, A.; Sly, W. S.; Christianson, D. W. Crystal structure of the secretory form of membrane-associated human carbonic anhydrase IV at 2.8 Å resolution. *Proc. Natl. Acad. Sci. U.S.A*. **1996**, *93*, 13589–13594.
(25) (a) Kannan, K. K.; Ramanadham, M.; Jones, T. A. Structure, refinement, and function of carbonic anhydrase isozymes: refinement of human carbonic anhydrase I. *Ann. N.Y. Acad. Sci*. **1984**, *429*, 49–60. (b) Eriksson, A. E.; Jones, T. A.; Liljas, A. Refined structure of human carbonic anhydrase II at 2.0 Å resolution. *Proteins* **1988**, *4*, 274–282. (c) Alterio, V.; Hilvo, M.; Di Fiore, A.; Supuran, C. T.; Pan, P.; Parkkila, S.; Scaloni, A.; Pastorek, J.; Pastorekova, S.; Pedone, C.; Scozzafava, A.; Monti, S. M.; De Simone, G. Crystal structure of the extracellular catalytic domain of the tumor-associated human carbonic anhydrase IX. *Proc. Natl. Acad. Sci. U.S.A*. **2009**, *106*, 16233–16238.
(26) (a) Alterio, V.; Di Fiore, A.; D'Ambrosio, K.; Supuran, C. T.; De Simone, G. X-Ray crystallography of CA inhibitors and its importance in drug design. In *Drug Design of Zinc−Enzyme Inhibitors: Functional, Structural, and Disease Applications*; Supuran, C. T., Winum, J. Y., Eds.; Wiley: Hoboken, 2009; pp 73−138; (b) Supuran, C. T. Carbonic anhydrase inhibitors. *Bioorg. Med. Chem. Lett*. **2010**, *20*, 3467–3474.
(27) Khalifah, R. G. The carbon dioxide hydration activity of carbonic anhydrase. I. Stop-flow kinetic studies on the native human isoenzymes B and C. *J. Biol. Chem*. **1971**, *246*, 2561–2573.
(28) Oxford Diffraction. *CrysAlis RED, version 1.171.32.2*; Oxford Diffraction Ltd, 2006.
(29) Jones, T. A.; Zhou, J. Y.; Cowan, S. W.; Kjeldoard, M. Improved methods for building protein models in electron density maps and the location of errors in these models. *Acta Crystallogr., Sect. A: Found. Crystallogr*. **1991**, *47*, 110–119.
(30) Brünger, A. T.; Adams, P. D.; Clore, G. M.; De Lano, W. L.; Gros, P.; Grosse-Kunstleve, R. W.; Jiang, J. S.; Kuszewski, J.; Nilges, M.; Pannu, N. S.; Read, R. J.; Rice, L. M.; Simonson, T.; Warren, G. L. Crystallography and NMR system: a new software suite for macromolecular structure determination. *Acta Crystallogr., Sect. D: Biol. Crystallogr*. **1998**, *54*, 905–921.
(31) Laskowski, R. A.; MacArthur, M. W.; Moss, D. S.; Thornton, J. M.; Thornton, J. M. PROCHECK—a program to check the stereochemical quality of protein structures. *J. Appl. Crystallogr*. **1993**, *26*, 283–291.
(32) O'Sullivan, M. C.; Dalrymple, D. M. A one step procedure for the selective trifluoroacetylation of primary amino groups of polyamines. *Tetrahedron Lett*. **1995**, *36*, 3451–3452.
(33) O'Sullivan, M. C.; Zhou, Q.; Li, Z.; Durham, T. B.; Ratendi, D.; Lane, S.; Bacchi, J. C. *Bioorg. Med. Chem*. **1997**, *5*, 2145–2155.